Research on Chemical Intermediates
https://doi.org/10.1007/s11164-025-05694-2

Synthesis, crystal structure, and electrochemical properties of 5-benzoyl-6-phenyl-pyrimidin-4-one-2-thione compound; voltammetric, spectrophotometric, and molecular docking studies of its interaction with DNA

Nida Nur Adiyan[1] · Abdulkadir Levent[2] · Şerife Pınar Yalçın[3] · Mehmet Sönmez[4]

Received: 16 May 2025 / Accepted: 10 July 2025

Abstract

A novel heterocyclic compound, 5-benzoyl-6-phenyl-pyrimidin-4-one-2-thione (PT), was synthesized for the first time via the cyclocondensation reaction of dibenzoyl acetic acid-N-carboxymethylamide with thiourea. The structure of the compound was characterized using elemental analysis, FT-IR, NMR, X-ray crystallography, and API-ES mass spectrometry. Electrochemical behavior of PT was investigated by cyclic voltammetry on a glassy carbon electrode in an anhydrous medium (0.1 M TBAP), revealing an irreversible cathodic peak at − 0.83 V, indicative of irreversible redox behavior and surface interaction. The interaction between PT and DNA was explored using voltammetric, spectrophotometric, and molecular docking techniques. Differential pulse voltammetry demonstrated a concentration-dependent decrease in the guanine oxidation signal, with a calculated binding free energy of − 6.5 kcal/mol. Spectrophotometric studies further supported the occurrence of a stable PT–DNA complex. Molecular docking revealed a strong binding affinity (− 8.12 kcal/mol), suggesting minor groove and electrostatic interaction modes. The consistency among electrochemical, spectroscopic, and computational findings indicates that PT forms a thermodynamically favorable and specific interaction with DNA. These results provide a foundation for future research on the therapeutic potential of PT and related pyrimidine thione derivatives.

Extended author information available on the last page of the article

Published online: 22 July 2025

Graphical abstract

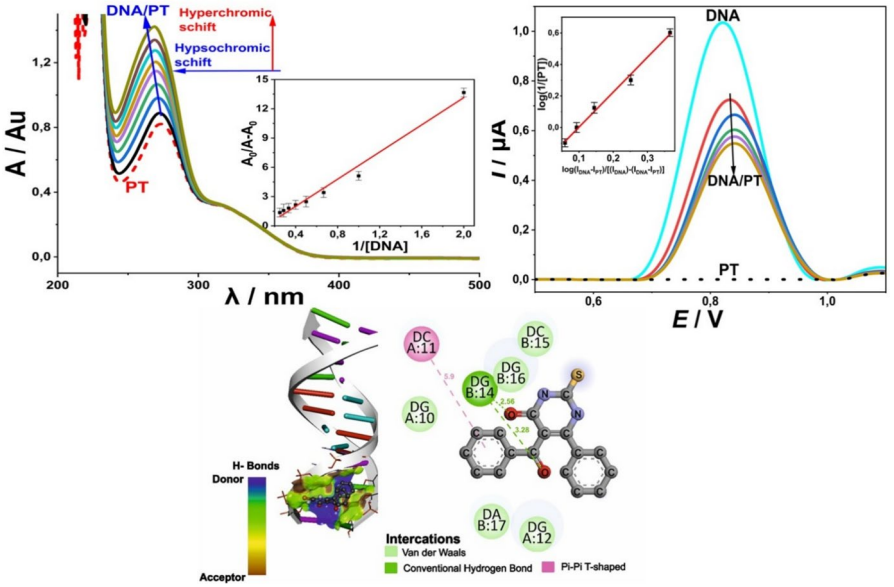

Keywords Pyrimidine thione · X-ray crystallography · DNA · Voltammetry · Spectrophotometric · Molecular docking

Introduction

Heterocyclic compounds, known to have various biological activities, have an important place in medicinal chemistry due to their therapeutic and pharmacological properties [1]. These compounds are present in many drugs, antibiotics, vitamins, natural products, and many biomolecules. Nitrogenous bases form the framework for many basic biomolecules. Pyrimidine and purine pharmacophores are the basic structural elements in molecules such as DNA and RNA, which contain genetic information and have basic components of nucleic acids, and are involved in various biological activities such as cell signaling [1]. They are widely found in nature as N-substituted sugar derivatives (nucleosides) and in vitamin B1 [2]. Many researchers have published about the synthesis and properties of pyrimidine and related compounds [3–7]. When these studies are examined, pyrimidine derivatives can be synthesized by many different methods. Pyrimidine thiones, which are heterocyclic compounds, also have biological importance. The structural interactions of thioxopyrimidine derivatives with purine bases such as adenine and guanine are frequently discussed in the literature. Various studies reported that pyrimidine thione derivatives exhibit many biological activities, including antimicrobial, anti-inflammatory, antihypertensive, antidiabetic, antibacterial, antifungal, antitumor,

antioxidant, and antiviral activities [8–12]. In particular, 5-fluorouracil and its modified analogue, 5-fluorothiouracil, are widely used anticancer agents. These drugs can insert into RNA and/or DNA and interfere with the maturation of nuclear RNA and/or DNA [13]. In addition, a study reported that some pyrimidine-2-thione derivatives might be used as an attractive antitumor agent with future clinical applications for the treatment of breast cancer due to their antineoplastic activity via inhibition of p-JNK protein in cancer cells [14].

As mentioned above, pyrimidine derivatives were proven to be an important structure in medicinal chemistry due to their wide biological and pharmacological activities [1, 3, 9, 13, 14]. In this study, a new thiouracil derivative, 5-benzoyl-6-phenyl-pyrimidin-4-one-2-thione (PT), was synthesized for the first time by a simple synthesis technique. The structural diversity of pyrimidine derivatives allows their interaction with biological macromolecules, and this feature makes them promising candidates for deeper investigation of their molecular mechanisms. In addition to their biological relevance, heteroatomic compounds such as pyrimidines and thiones have been widely studied electrochemically using cyclic voltammetry (CV), due to their redox-active centers and π-conjugated systems. CV is a valuable tool for evaluating the electron transfer properties, adsorption behaviors, and reaction kinetics of such molecules at various electrode surfaces [5, 6, 15, 16]. Pyrimidine-based compounds, owing to their nitrogen and sulfur heteroatoms, show characteristic irreversible or quasi-reversible redox behavior depending on substitution patterns, electrolyte composition, and scan rate [17]. Many studies report that these heterocycles may undergo surface adsorption, chemical transformation, or electrochemical reduction/oxidation, often forming films or intermediates on electrode surfaces [18–21]. The shift in peak potentials and variation in current response with scan rate has been particularly useful in characterizing diffusion-controlled or adsorption-assisted mechanisms in heteroatomic structures [22]. Such findings underline the importance of voltammetric studies in understanding the electrochemical reactivity and interaction potential of pyrimidine-based molecules with biological or electrode environments. In this context, the investigation of the redox behavior of the newly synthesized PT compound using CV contributes to the growing body of knowledge on heteroatomic molecular systems and their electrochemical characteristics.

Understanding the mechanisms by which small molecules interact with DNA has vital importance, particularly for the development of anticancer drugs [23–25]. Interactions with DNA can cause molecules to alter the structure and function of DNA through various mechanisms, such as intercalation, groove binding, or electrostatic interactions [13, 24, 26–29]. These interactions often affect cellular processes such as replication and transcription, forming the basis of biological activity. Molecular docking studies provide an atomic-level understanding of where and how a molecule binds to DNA. This method supports experimental data by analyzing both binding energies and specific interaction sites, providing important guidance for the design of new therapeutic agents [24, 30–32].

Electrochemical techniques are the most powerful techniques for studying interactions with DNA [24, 33–35]. Voltammetric studies allow evaluation of whether a molecule interacts with DNA by examining its redox behavior and of how these interactions change the redox properties of the molecule [24, 36, 37].

Spectrophotometric methods complete this process by revealing the binding mode of the molecule with DNA and its binding constants [38–41]. In this study, the synthesis, X-ray crystallography characterization, and electrochemical properties of a new PT compound were investigated. In addition, the interaction of the compound with DNA was evaluated using voltammetric and spectrophotometric techniques, and the binding behavior was modeled in detail at the atomic level by molecular docking studies. Molecular docking analyses provide critical information to evaluate the potential of the compound as a therapeutic agent by elucidating the specific sites where the compound binds to DNA and the binding mechanism.

Experimental

Apparatus and chemicals

All chemicals used in this study were obtained commercially and used without purification. Deoxyribonucleic acid from fish sperm (DNA) was purchased from Sigma-Aldrich (74,782). Dibenzoyl acetic acid-N-carboxymethylamide (DBANMA) [42] was prepared according to the method given in the literature. Elemental analysis values were recorded with the Thermo Scientific Flash 2000 brand and model elemental analyzer. ^{1}H and ^{13}C NMR spectra were recorded with the Bruker High Performance Digital FT-NMR (600 MHz) spectrometer by dissolving the compound in d6-DMSO and using TMS as an internal standard (Figure SI 2 and Figure SI 3). The Perkin Elmer Spectrum 100 FT-IR Spectrometer (ATR) model was used to examine the FT-IR spectrum of the compound in the range of 4000–400 cm^{-1}. The mass spectrum of 5-benzoyl-6-phenyl-pyrimidin-4-one-2-thione was obtained by atmospheric pressure ionization electrospray mass spectra (Figure SI 4) (API-ES) on an LC–MS/MS ABSciex 3200 Q-trap spectrophotometer.

Synthesis of 5-benzoyl-6-phenyl-pyrimidin-4-one-2-thione

For this, 1 mmol DBANMA and 1 mmol thiourea were mixed well in a 50 mL reaction flask and then subjected to a direct reaction without solvent in an oil bath at 160 °C for 25 min. The oily product obtained was first treated with dry diethyl ether to obtain a solid product and then crystallized from n-butanol and saved in a desiccator (Figure SI 1). Yield: 64%; Mp: 215–216 °C. $C_{17}H_{12}O_2N_2S$ 308.13 g/mol. Theoretical: C: 66.23; H: 3.89; N: 9.09; S: 10.40. Found: C: 66.22; H: 4.00; N: 8.97; S: 10.35%. FT-IR(ATR) v, cm^{-1}: 3061 (NH), 2930 (C-HAr), 1678, 1637(C=O), 1595–1557 (C=C)phenyl, 1232,741 (C=S). ^{1}H NMR (600 MHz, DMSO) δ, ppm. 12.85 (s, 1H, NH), 12.81 (s, 1H, NH), 7.86 (d, J = 7.3 Hz, 2H, aromatic proton), 7.57 (t, J = 7.4 Hz, 1H, aromatic proton), 7.42 (t, J = 7.7 Hz, 2H, aromatic proton), 7.34 (tt, J = 14.8, 7.4 Hz, 5H, aromatic proton). ^{13}C NMR (151 MHz, DMSO) δ ppm. 192.40 (C=O) benzoyl), 176.45 (C=S), 159.97 (C=O) pyrimidine, 152.74, 137.29,

134.19, 131.09, 130.91, 129.63, 129.15, 128.93, 128.67, 116.31 (10 aromatic carbons). Mass: Calculated Mass = 308.13, Observed m/z = 307.05 $[M]^+$ mode.

X-ray crystallography

The single-crystal X-ray data of $C_{17}H_{12}N_2O_2S$ compound were collected on a Bruker/D8 QUEST diffractometer by the ω-scanning technique using graphite-monochromatic MoKα radiation (λ, 0.71073 Å) at 293 K. The structure was solved by direct methods using SHELXS implement in WINGX [43] program suit. The program ORTEP-3 for Windows [44] was used in the preparation of the molecular graphics. The refinement was carried out by Direct Methods method using SHELXL [45]. X-ray crystallographic data are listed in Table SI 1. Bond distances and angles are given in the supplementary documents (Table SI 2).

Voltammetric method

Electrochemical properties of PT were investigated using the Autolab PGSTAT 128N potentiostat (Netherlands) and a triple cell stand (BASi). Glassy carbon (GC, Φ: 3 mm, BASi), Ag/AgCl (BASi), and Pt (BASi) wires were used as the working electrode, reference electrode, and auxiliary electrode in voltammetric experiments, respectively. For experiments, 1 mM PT was prepared in DMSO (supporting electrolyte solution containing 0.1 M tetrabutylammonium perchlorate (TBAP)). Before each voltammetric analysis, the surface of the GC electrode was cleaned manually. In studies in an anhydrous environment, pure nitrogen gas was passed through the solution for 10 min before the analyses.

Voltammetric measurements of PT in aqueous medium: Cyclic voltammograms were recorded in the potential range of − 1.2 to 1.0 V in DMSO medium containing 1 mM PT and 0.1 M TBAP on the GC electrode.

DNA immobilization on the GC electrode surface: For this, 25 mg/L DNA was immobilized on the GC electrode in phosphate buffer (PBS, pH 7.4, containing 0.02 M NaCl) medium at a voltage of + 0.50 V for 120 s.

Interaction with PT–DNA: After DNA was immobilized on the GC electrode surface, 1 mg/L PT was left in PBS (pH 7.4 containing 0.02 M NaCl) medium for periods ranging from 5 to 150 s.

Voltammetric measurement: After the interaction of PT with DNA, voltammograms were recorded in the voltage range of + 0.5 to + 1.40 V using the differential pulse technique.

Spectrophotometric technique

The spectra for PT, DNA, and PT–DNA interaction were recorded in the wavelength range of 200–800 nm with a Shimadzu Pharma Spec UV-1900 spectrophotometer. Spectral measurements of the compounds were carried out in PBS (pH 7.4) medium.

Docking measurements

The two-dimensional structure of PT was drawn with the ChemDraw Ultra program and then converted to pdb files. The 3-dimensional crystal structure of DNA (PDB ID: 1BNA) was obtained from the RCSB database (http://www.rcsb.org/pdb). DNA and grid preparations were made with the help of the AutoDock_vina_1.1.2 program. In this process, water molecules in the DNA file were deleted. After the polar hydrogen atoms were added, Gustier charging was performed. The docking file for the PT compound was prepared in the same way, and molecular docking operations were performed with the AutoDock_vina_1.1.2 program [30]. DNA was placed in AutoDock Tool 4.2 by creating a PDBQT file containing a protein with hydrogens in all polar groups. The grid area of 14.74, 20.98, and 8.80 dimensions was created for the docking site on the target DNA. The Discovery Studio 4.0 program processor was used to create hydrogen bonds and hydrophobic interactions in the PT–DNA interaction.

Results and discussion

Synthesis and characterization of 5-benzoyl-6-phenyl-pyrimidin-4-one-2-thione compound

In this study, for the first time, PT compound was obtained by the reaction of dibenzoyl acetic acid-N-carboxymethyl amide and thiourea in a solvent-free environment at 160 °C in an oil bath for 25 min, as stated in the synthesis section (Figure SI 1). The synthesized PT compound was purified by crystallization from n-BuOH after washing several times in methanol. Elemental analysis, FT-IR, $^{1}H/^{13}C$ NMR (Figure SI 2-4) and LC–MS/MS spectral values (Figure SI 5) were used for the characterization of the compound. When the IR spectrum of the PT compound is compared with the spectrum of substituted pyrimidine-2-thion ring compounds in the literature, it is seen that the bands belonging to specific groups vibrate in similar regions. When the FT-IR spectrum (Figures SI 2) of the PT compound was examined, as expected, bands belonging to NH vibrations at 3060 cm^{-1} and C=O vibrations at 1678 and 1637 cm^{-1} were observed [46]. The C=C stretching vibrations in the phenyl rings attached to the pyrimidine ring vibrate at 1595–1557 cm^{-1}. Again, vibrations belonging to the thione group were observed at 1237 and 741 cm^{-1}, supporting the synthesized structure [46–48].

As shown in Figures SI 2 and 3, the ^{1}H NMR and ^{13}C NMR spectra of the compound were examined in d6-DMSO at room temperature, respectively. The ^{1}H NMR spectrum of the pyrimidine compound showed signals as singlets at $\delta = 12.81$ and 12.85 ppm, corresponding to NH signals. Signals corresponding to aromatic protons appeared between $\delta = 7.34$–7.82 ppm. The ^{13}C NMR spectrum showed characteristic signals at 192.40, 176.45, and 159.97 ppm due to O=C–Ar, C=S, pyrimidine, and C=O, pyrimidine ring of the compound, respectively [48]. It showed 10 peaks in the region of 152.74–116.31 ppm due to other aromatic carbon atoms. Because of the symmetry of some carbons in the phenyl

and benzoyl rings are identical and give one peak. Namely; C7 with C9 and C10 with C6 are identical in the phenyl ring give a peak at 129.63 and 129.15 ppm. Similarly, C18 with C22 and C19 with C21 in the benzoyl ring are the identical and give a peak at 128.93 and 128.67 ppm. All analytical and spectroscopic data obtained support the proposed structure.

The ORTEP-3 diagram of the title compound is presented in Fig. 1. The molecule crystallizes in the monoclinic space group P21/c, with the following dimensions: $a = 16.299(4)$, $b = 7.906(2)$, $c = 11.836(3)$, and $\beta = 104.3$ (9) (Table SI 1).

The carbon–carbon bond lengths range from 1.37(2) to 1.50(2) Å, with the C12–C15 and C14–C15 bonds in the PT observed at 1.38 and 1.46 Å, respectively (Table SI 2). Additionally, the carbon–sulfur bond length is measured at 1.67(3) Å, consistent with the findings of Fabijanić et al. (2017) [49]. The C–N bond length varies between 1.362 and 1.396 Å, which is shorter than the typical C–N single bond length of 1.48 Å but slightly longer than the expected C=N double bond length of 1.28 Å [50].The C–O bond length is observed in the range of 1.23(2) Å. The angle between plane centroids have been found about 76.6°. So, the overall structure deviates from planarity. This indicates that, while parts of the molecule (such as aromatic or unsaturated rings) may be locally planar, the molecule adopts a twisted conformation.

The angle around C–C bonds have been found around 120°. The reported angles of around 120° are characteristic of sp^2 hybridization, common in planar regions like aromatic rings. The crystal packing diagram of the title compound can be seen in Fig. 2 (CCDC deposition number is 2,432,561). The geometry tools allow for distance and angle measurements, which would be useful in confirming N–H···S and C–S···H interactions as discussed earlier [49].

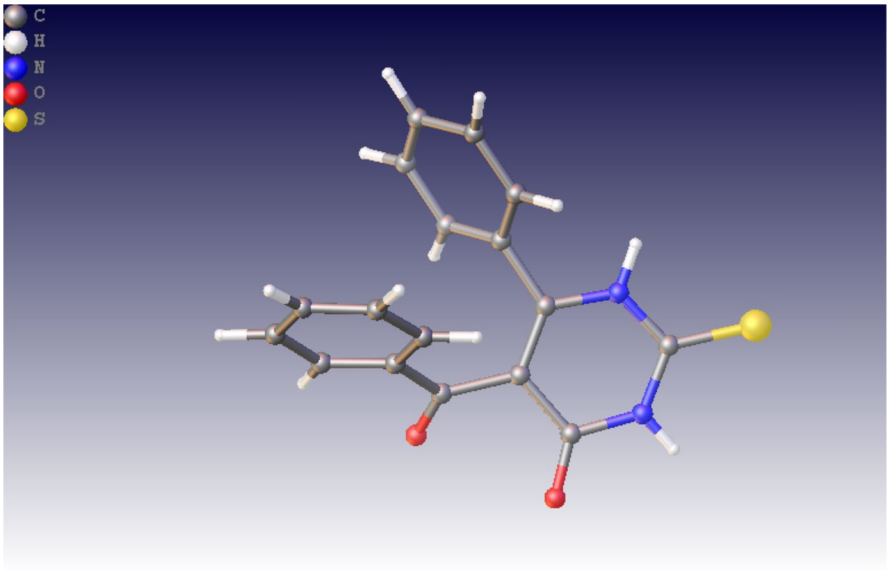

Fig. 1 The Ortep view of the PT compound

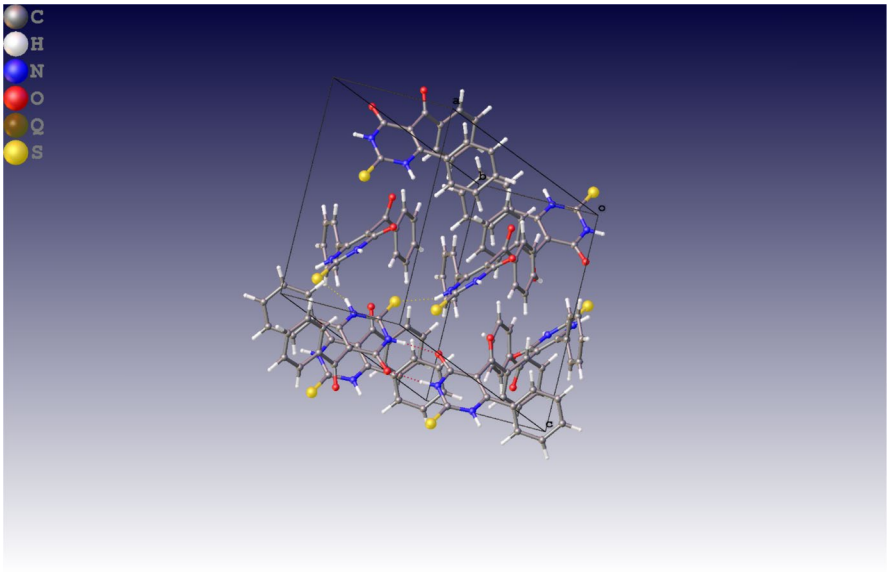

Fig. 2 The crystal packing of the PT compound

Cyclic voltammetry results of 5-benzoyl-6-phenyl-pyrimidin-4-one-2-thione compound on GCE

Cyclic voltammetry results of the PT compound on GCE in anhydrous medium (0.1 M TBAP) are given in Fig. 3. In Fig. 3a, an irreversible cathodic peak was observed around −0.83 V in three-cycle CV curves at a 100 mV/s voltage scan rate. A higher current density is observed in the first cycle, which indicates that there is

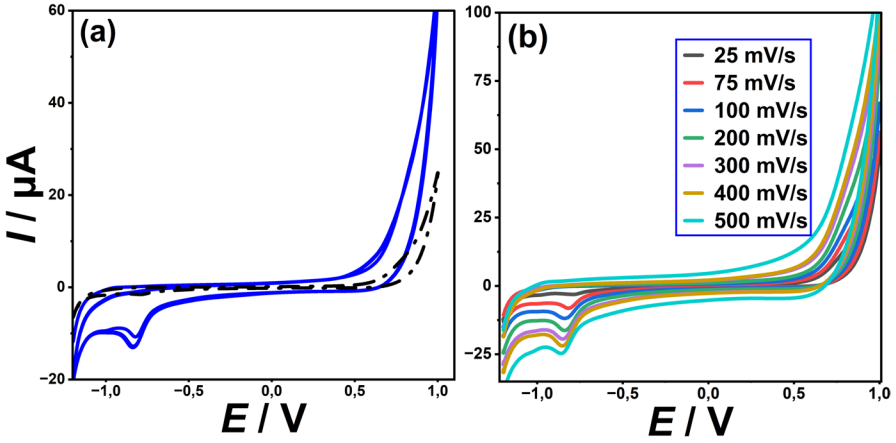

Fig. 3 Cyclic voltammetry curves for the PT compound recorded on GCE at **a** 100 mV/s voltage scan rate and **b** 25 mV/s and 500 mV/s voltage scan rates. Dashed line: 0.1 M TBAP supporting electrolyte

adsorption or chemical transformation on the electrode surface. The decrease in current density after the first cycle can be attributed to reasons such as the binding of the compound to the electrode surface or the formation of a surface film. How the reaction kinetics change with increasing scan rates is clearly observed. At low rates, the reaction is more balanced, but at high rates, kinetic and diffusion effects become dominant. In addition, the cathodic peak voltage value shifted to more negative values as the voltage scan rate increased (Fig. 3b). The linear relationship between the cathodic peak current value, the voltage scan rate and the slope value between the logarithm of the cathodic peak current value and the voltage scan rate logarithm (0.678) were calculated between 0.5 and 1. These results show that PT has a diffusion-assisted adsorption feature on GCE under these study conditions.

Voltammetric results for the interaction of PT compound with DNA

Voltammetric studies of the PT–DNA interaction were carried out as stated in section (voltammetric method). In these studies, firstly, the conditions were identified under which the anodic signal intensity of the guanine base on GCE of DNA was most sensitive. For this purpose, researchers generally use the DPV technique as a voltammetric technique in drug-DNA interaction studies [24, 36]. Thus, optimization experiments were carried out for the guanine anodic signal. Deposition voltage (0 to + 0.6 V) and deposition time (0–210 s) for the guanine signal in PBS supporting electrolyte (pH 7.4, containing 0.02 M NaCl) were studied. As a result of the experiments, the most sensitive signals were obtained at 120 s deposition time and + 0.5 V deposition voltage values on GCE (Fig. 4, black line). Under these study conditions, a 65% increase in guanine anodic signal intensity and a positive change in anodic voltage value were observed in the interaction of the PT compound with DNA (Fig. 4, dashed red line). The changes in guanine oxidation signal upon addition of PT compound suggest a strong interaction between PT and the guanine moiety of DNA. Guanine bases are electroactive and provide a measurable anodic peak due to their oxidation at the electrode surface. A decrease in the guanine oxidation peak current after PT addition indicates that PT likely binds to DNA and hinders the electron transfer of guanine. This is commonly observed in intercalative or electrostatic interactions, where drug molecules occupy binding sites between base pairs or on the phosphate backbone, respectively, reducing the accessibility of guanine for oxidation [22, 51, 52].

In this part of the study, DPV curves were recorded between 5 and 150 s in order to determine the maximum interaction time for the interaction of DNA with PT (Fig. 5). The anodic signal intensity in the guanine base of DNA decreases as the interaction time increases. In this process, a decrease in the anodic signal intensity was detected due to the complex structure formed between DNA and PT. There was no significant change in the anodic signal intensity after 90 s due to the interaction between DNA and PT. Thus, the interaction time was accepted as 90 s unless otherwise stated in the following parts of the analytical study (Fig. 6).

In the optimum conditions of this study, DPV curves were recorded by adding PT between 0.25 mg/L and 1.25 mg/L while keeping the DNA concentration constant

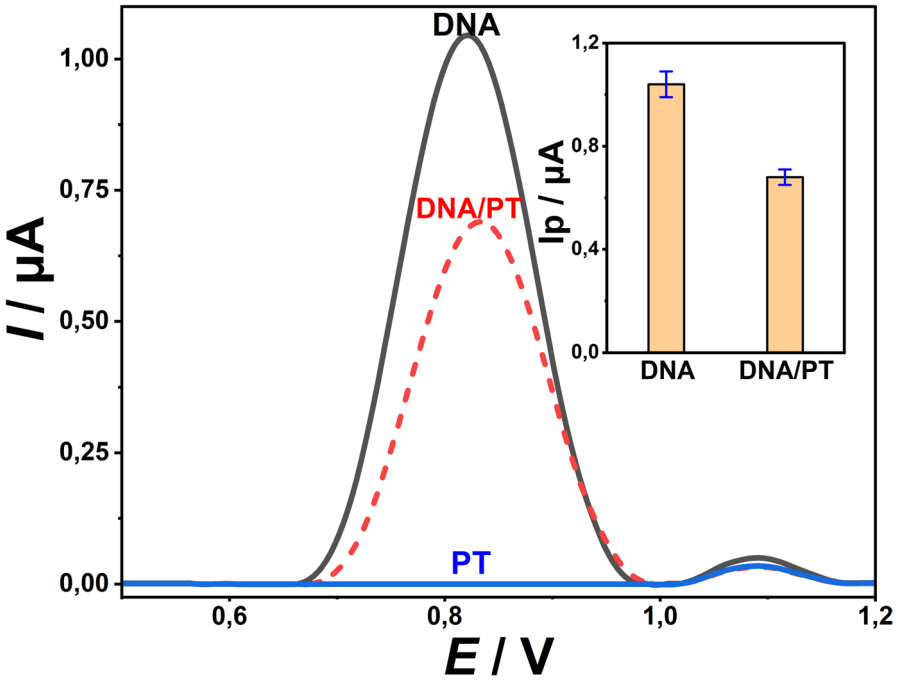

Fig. 4 Differential pulse voltammograms recorded in PBS (pH 7.4, containing 0.02 M NaCl) supporting electrolyte medium for PT–DNA interaction

at 25 mg/L in PBS (pH 7.4, containing 0.02 M NaCl) medium (Fig. 6). As can be seen from the recorded DPV curves, a decrease in the anodic signal intensity was observed due to the PT–DNA complex compound formed after each PT addition. This behavior is consistent with drug-DNA interactions observed for many small molecules, where the binding of the drug alters the structural conformation of DNA and restricts the electrochemical accessibility of nucleobases [51, 53]. Analytically, there was no significant change after the addition of 1.25 mg/L PT. The anodic peak voltage value shifted to a more positive region due to the PT–DNA interaction. The interaction of PT with DNA has great importance in terms of determining the binding constant. This binding constant shows how effectively PT enters and binds to the target cells of DNA. As a result of this interaction, the formation of a PT + DNA ↔ PT–DNA complex structure was evaluated as a simple model. The binding constant was calculated from the recorded PT–DNA interaction curves according to the following Equation [54].

$$log\frac{1}{[PT]} = logK + log\frac{I_{(PT-DNA)}}{I_{DNA} - I_{(PT-DNA)}})$$

In the equation, K represents the binding constant, I_{DNA} guanine peak current and $I_{(\mathrm{PT–DNA})}$ represents the guanine peak current measured after the interaction of PT with DNA. The binding constant K of this complex was found using the value where

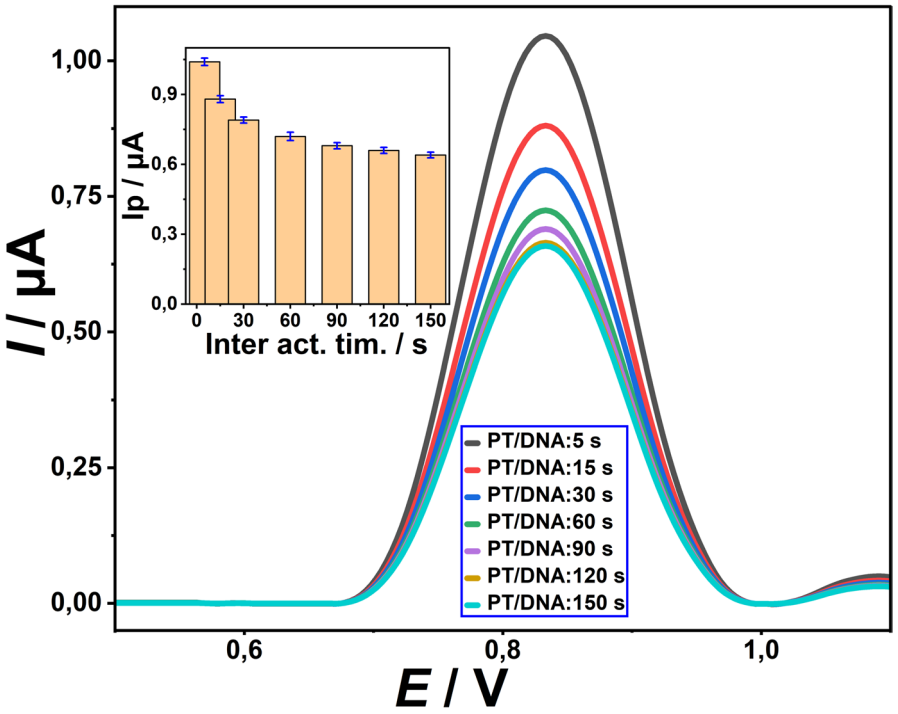

Fig. 5 Differential pulse voltammograms recorded for PT–DNA interaction time

the y-axis intersects the curve obtained by plotting log(1/[PT]) against log(I_{PT-DNA}/ $I_{DNA} - I_{(PT-DNA)}$) values. The Kb constant between PT and DNA was found to be $1.05 \times 10^{+5}$. The free energy of binding was calculated as $\Delta G = -$RTInKb, where $\Delta G = -6.50$ kcal/mol. A negative ΔG value indicates that the PT–DNA binding process is spontaneous under the studied conditions. Furthermore, the positive shift in peak potential and suppression of guanine oxidation signal suggest that the PT molecule may interact with DNA via intercalation or electrostatic binding, which are typical mechanisms for small-molecule-DNA interactions. Intercalators usually insert between base pairs, while electrostatic interactions often occur along the negatively charged phosphate backbone [22, 24, 51]**.** The fact that AG < 0 indicates that the PT–DNA complex structure interaction can occur spontaneously on the GCE surface under these working conditions. As can be seen from this interaction, the PT compound probably interacted with DNA via electrostatic interaction or intercalation [25]. In this process, the charge transfer force of the PT compound can intervene between the helical structures of DNA and deform the DNA.

Spectrophotometric results for PT–DNA interaction

Firstly, the spectra were recorded for the PT compound in the wavelength range of 200–800 nm (Fig. 7, red dashed line). PT gave a well-defined maximum absorption

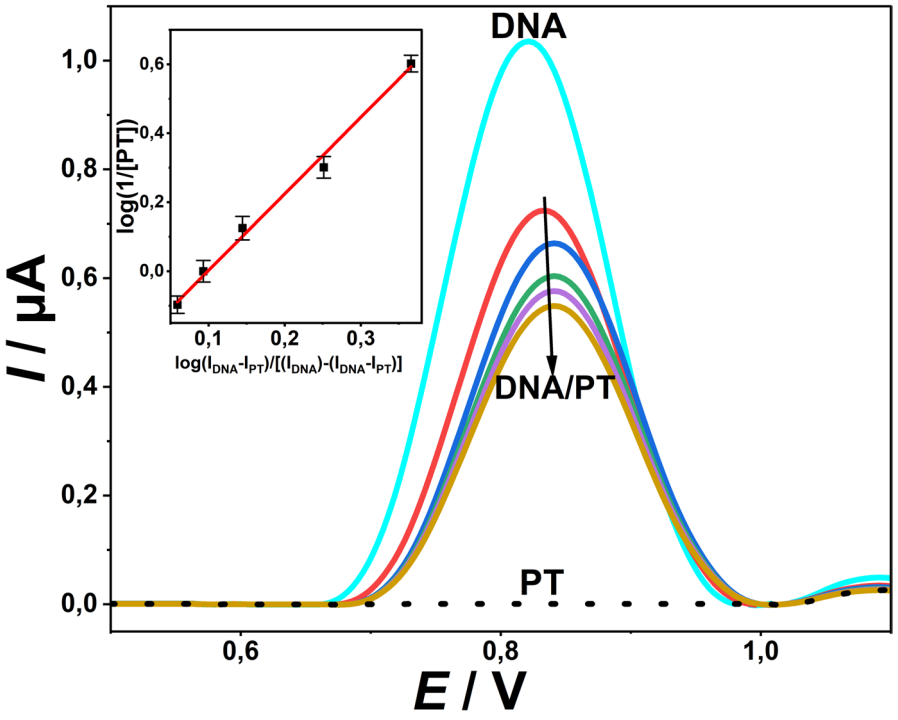

Fig. 6 Differential pulse voltammograms recorded in PBS (pH 7.4, containing 0.02 M NaCl) supporting electrolyte medium using GCE for PT–DNA interaction

band at 274 nm and a very broad-spectrum wave at approximately 325 nm. In the interaction experiments of PT with DNA, the spectra for the complex compound formed after adding 0.5–4 mg/L DNA to the PT solution were recorded in the wavelength range of 200–800 nm in PBS (pH 7.4) medium (Fig. 7). In these experiments, no analytical change was observed in the spectral band observed at approximately 325 nm wavelength after each successive addition of DNA solution. However, in the absorption band observed at 274 nm wavelength, there was an increase in absorbance intensity (hyperchromic shift) and a shift in wavelength toward 269 nm (hypochromic shift) due to the complex compound structure formed after each DNA addition.

The increase in absorption during the interaction of PT with DNA indicates that the local structure of DNA is disrupted or base pairs are exposed. This is usually associated with denaturation of DNA or binding of PT to major/minor grooves of DNA. At the same time, hypochromism is caused by the overlapping of π electrons due to the insertion of functional groups from PT between DNA base pairs (intercalation), and these data are also consistent with molecular docking data [55, 56]. In addition, the shift in wavelength, the change in absorption intensity, and the isobestic point observed at 325 nm wavelength indicate that a new complex structure formed as a result of the interaction of the PT compound with DNA. The binding

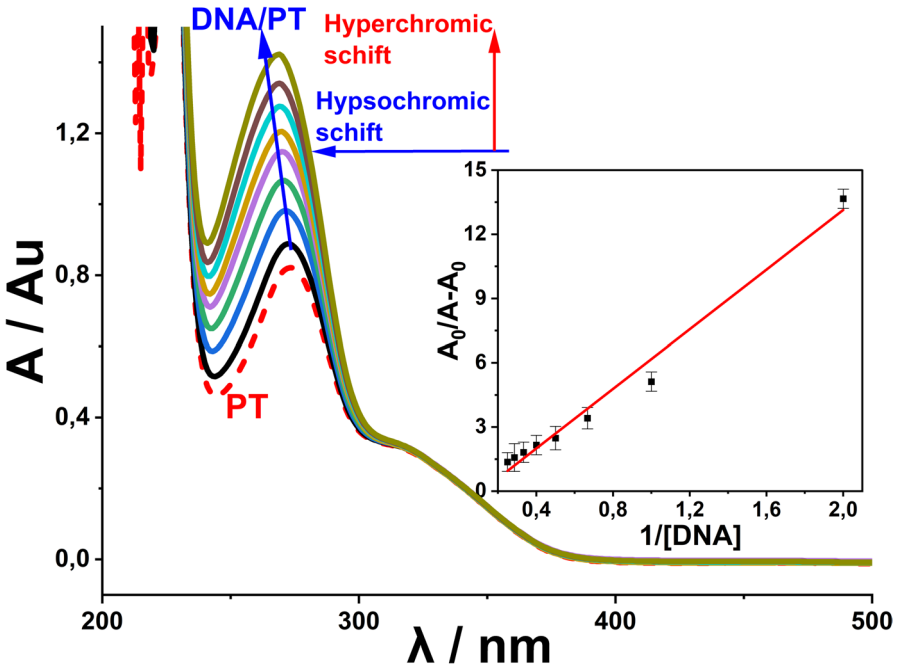

Fig. 7 Spectrophotometric spectra recorded for the interaction of PT with DNA

constant (K) of this complex compound was calculated using the Benesi-Hildebrand equation ($\frac{A_0}{A-A_0} = \frac{\varepsilon_G}{\varepsilon_{H-G}} + \frac{\varepsilon_G}{\varepsilon_{H-G}-\varepsilon_G} x \frac{1}{K[DNA]}$) [57]. Here A_0 is the absorbance of PT, A is the absorbance of PT–DNA complex, $\mathscr{E}$ is the PT absorption coefficient, and $\mathscr{E}_{H\text{-}G}$ is the absorption coefficient of the PT–DNA complex. When the necessary calculations were made, $K = 1.19 \times 105\ M^{1-}$ was found. By using the PT–DNA complex formation constant, the binding free energy (ΔG) was calculated as $\Delta G = -6.35$ kcal/mol. These results show that the interaction with PT–DNA causes the hypochromism effect in the absorption spectrum of DNA [27, 55]. These interactions show that the compound binds to DNA via intercalation and groove binding, which is consistent with the molecular docking results.

Molecular docking results for PT–DNA interaction

Molecular docking studies are a powerful computational technique used to understand and model interactions between biomolecules. This technique provides useful preliminary information, especially for studies in the field of drug design. Molecular docking is used to model how potential drug candidates will bind to biomolecules such as target proteins, DNA, or RNA. The evaluation of the obtained data contributes to the understanding of target-drug interactions in the drug development process. As a result of docking studies, whether biomolecular targets are suitable for drug development can be checked. The molecular docking results for the PT–DNA

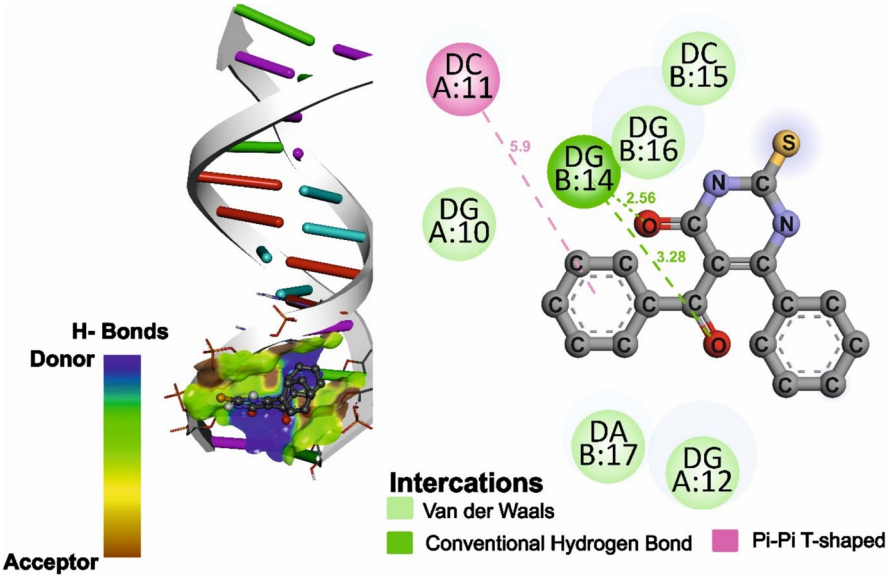

Fig. 8 Molecular docking images and results recorded for PT–DNA interaction

interaction are given in Fig. 8. In this computational simulation, two strong interactions were observed. DNA DG B:14 nucleotides made conventional hydrogen bonds with the oxygen in the pyrimidine carbon at an average distance of 5.56 Å and with the oxygen at the benzoyl carbon at an average distance of 7.78 Å. At the same time, DC A:11 nucleotide interacted with the benzoyl phenyl ring and formed a Pi-donor hydrogen bond [58]. These interactions were connected with a binding affinity of −8.12 kcal/mol. The molecular docking binding affinity is compatible with both voltammetric and spectrophotometric results. The PT–DNA interaction appears to involve electrostatic and minor groove binding.

Conclusion

In this study, we synthesized a new heterocyclic compound PT, and its structural characterization was successfully carried out by methods such as microanalysis, FT-IR, NMR, API-ES, and X-ray crystallography. Voltammetric studies using GCE showed that PT gave an irreversible reduction peak at −0.83 V, which revealed the electrochemical stability of the compound and its irreversible redox behavior.

Interaction studies with DNA showed that PT had a strong and thermodynamically favorable binding process with DNA. Voltammetric analysis results calculated the binding free energy as −6.5 kcal/mol, and the results obtained from spectrophotometric and molecular docking studies supported these findings. Molecular docking data determined the binding free energy as −8.12 kcal/mol and revealed that PT interacted with DNA electrostatically and via the minor binding groove. The

findings demonstrate the potential of PT to interact with biomolecules and particularly its ability to bind with DNA, suggesting that compounds synthesized based on PT may be candidates for therapeutic and biomedical applications in the future.

Supplementary Information The online version contains supplementary material available at https://doi.org/10.1007/s11164-025-05694-2.

Author contributions Nida Nur Adiyan: Conceptualization, Software, Writing—original draft. Şerife Pınar Yalçın: Data curation, Investigation, Writing—original draft. Abdulkadir Levent: Methodology, Writing—original draft, Writing—review & editing, Supervision. Mehmet Sönmez: Data curation, Methodology, Writing—original draft. All authors read and approved the final version of the manuscript.

Data availability The data that support the findings of this study will not be made publicly available. No datasets were generated or analysed during the current study.

Declarations

Ethical approval Safety data retrieved from the spontaneous reporting process are anonymous and concur with ethical standards. Therefore, there was no further requirement for the ethical measure.

Conflict of interest All authors certify that they have no affiliations with or involvement in any organization or entity with any financial interest or non-financial interest in the subject matter or materials discussed in this manuscript. The authors declare no conflict of interests. The authors declare no competing interests.

References

1. F.O. Sefrji, A.F. Alrefaei, M.A. Imam et al., Synthetic approaches for novel fused pyrimidine derivatives: design, structural characterization, antiviral, antitumor, and molecular docking evaluation. Heliyon **10**, e40903 (2024). https://doi.org/10.1016/j.heliyon.2024.e40903
2. S. Bhilare, H. Shet, Y.S. Sanghvi, A.R. Kapdi, Discovery, synthesis, and scale-up of efficient palladium catalysts useful for the modification of nucleosides and heteroarenes. Molecules **25**, 1645 (2020). https://doi.org/10.3390/molecules25071645
3. M. Sönmez, M. Çelebi, A. Levent et al., Synthesis, characterization, cyclic voltammetry, and antimicrobial properties of N-(5-benzoyl-2-oxo-4-phenyl-2*H*-pyrimidine-1-yl)-malonamic acid and its metal complexes. J. Coord. Chem. (2010). https://doi.org/10.1080/00958972.2010.494252
4. E. Akbas, A. Levent, S. Gümüş et al., Synthesis of some novel pyrimidine derivatives and investigation of their electrochemical behavior. Bull. Korean Chem. Soc. (2010). https://doi.org/10.5012/bkcs.2010.31.12.3632
5. M. Sönmez, M.E. Hacıyusufoğlu, A. Levent et al., Synthesis of pyrimidine Schiff base transition metal complexes: characterization, spectral and electrochemical analyses, and photoluminescence properties. Res. Chem. Intermed. **44**, 5531–5546 (2018). https://doi.org/10.1007/s11164-018-3438-5
6. E. Ergan, E. Akbas, A. Levent et al., Synthesis, theoretical calculation, electrochemistry and total antioxidant capacity of 5-benzoyl-6-phenyl-4-(4-methoxyphenyl)-1,2,3,4-tetrahydro-2-thioxopyrimidine and derivatives. J. Mol. Struct. (2017). https://doi.org/10.1016/j.molstruc.2017.02.001
7. M. Sönmez, M. Çelebi, Y. Yardım, Z. Şentürk, Palladium(II) and platinum(II) complexes of a symmetric Schiff base derived from 2,6,diformyl-4-methylphenol with N-aminopyrimidine: synthesis, characterization and detection of DNA interaction by voltammetry. Eur. J. Med. Chem. **45**, 4215–4220 (2010). https://doi.org/10.1016/j.ejmech.2010.06.016
8. S.M. Rajesh, R.S. Kumar, L.A. Libertsen et al., A green expedient synthesis of pyridopyrimidine-2-thiones and their antitubercular activity. Bioorg. Med. Chem. Lett. **21**, 3012–3016 (2011). https://doi.org/10.1016/j.bmcl.2011.03.045

9. S. Rizk, M. El Sayed Alya, Practiced synthesis and biological evaluation of some new pyrimidin-2-thione derivatives as potential anticancer agents. Egypt. J. Chem. (2022). https://doi.org/10.21608/ejchem.2022.146115.6357
10. E. Żesławska, I. Korona-Głowniak, M. Szczesio et al., Structural analysis and antimicrobial activity of 2[1H]-pyrimidinethione/selenone derivatives. J. Mol. Struct. **1142**, 261–266 (2017). https://doi.org/10.1016/j.molstruc.2017.04.067
11. A.M. Srour, A.E.-H.A. Ismail, S.M. El-Kosy, Antiviral and antischistosomal evaluation of newly synthesized thioglycosides and their acyclic analogues. Z. Naturforsch. C **64**, 483–489 (2009). https://doi.org/10.1515/znc-2009-7-803
12. R. Soliman, H.M. Feid-Allah, H.F. Mohamed, Preparation and antidiabetic activity of cyclic sulfonylthiourea derivatives. J. Pharm. Sci. **70**, 952–956 (1981). https://doi.org/10.1002/jps.2600700834
13. A.M. El-Naggar, M.M. Abou-El-Regal, S.A. El-Metwally et al., Synthesis, characterization and molecular docking studies of thiouracil derivatives as potent thymidylate synthase inhibitors and potential anticancer agents. Mol. Divers. **21**, 967–983 (2017). https://doi.org/10.1007/s11030-017-9776-1
14. M.M. Salem, M.N. Gerges, A.A. Noser, Synthesis, molecular docking, and in-vitro studies of pyrimidine-2-thione derivatives as antineoplastic agents via potential RAS/PI3K/Akt/JNK inhibition in breast carcinoma cells. Sci. Rep. (2022). https://doi.org/10.1038/s41598-022-26571-7
15. M. Sönmez, M. Çelebi, A. Levent et al., Synthesis, characterization, cyclic voltammetry, and antimicrobial properties of *N* -(5-benzoyl-2-oxo-4-phenyl-2 *H* -pyrimidine-1-yl)-malonamic acid and its metal complexes. J. Coord. Chem. **63**, 1986–2001 (2010). https://doi.org/10.1080/00958972.2010.494252
16. R.G. Compton CEB. Understanding Voltammetry G - Reference,Information and Interdisciplinary Subjects Series. World Scientific (2007)
17. E. Laviron, General expression of the linear potential sweep voltammogram in the case of diffusionless electrochemical systems. J. Electroanal. Chem. Interfacial Electrochem. **101**, 19–28 (1979). https://doi.org/10.1016/S0022-0728(79)80075-3
18. H. Kiliç, M. Berkem, Electrochemical behavior of some new pyrimidine derivatives. J. Serb. Chem. Soc. **69**, 689–703 (2004). https://doi.org/10.2298/JSC0409689K
19. P. de-los-Santos-Álvarez, M.J. Lobo-Castañón, A.J. Miranda-Ordieres, P. Tuñón-Blanco, Electrochemistry of nucleic acids at solid electrodes and its applications. Electroanalysis **16**, 1193–1204 (2004). https://doi.org/10.1002/elan.200402995
20. P.D. Akrivos, Recent studies in the coordination chemistry of heterocyclic thiones and thionates. Coord. Chem. Rev. **213**, 181–210 (2001). https://doi.org/10.1016/S0010-8545(00)00372-6
21. B. Czochralska, M. Wrona, D. Shugar, Electrochemically reduced photoreversible products of pyrimidine and purine analogues, 133–181 (1986)
22. J. Wang, *Analytical Electrochemistry* (Wiley, 2006)
23. M. Sahadevan, M. Sundaram, K. Subramanian, Quantum mechanical approaches and molecular docking studies of metal based anticancer drugs *cis*-diammine glycolato platinum and diaminocyclohexane oxalatoplatinum structures. Comput. Biol. Chem. **106**, 107940 (2023). https://doi.org/10.1016/j.compbiolchem.2023.107940
24. M. Aslan, A. Levent, First voltammetric studies, spectrophotometric and molecular docking investigations of the interaction of an anticancer drug ribociclib-DNA and analytical applications of disposable pencil graphite sensor. Microchem. J. (2024). https://doi.org/10.1016/j.microc.2024.111580
25. M. Aslan, F. Aydın, A. Levent, Voltammetric studies and spectroscopic investigations of the interaction of an anticancer drug bevacizumab-DNA and analytical applications of disposable pencil graphite sensor. Talanta **265**, 124893 (2023). https://doi.org/10.1016/j.talanta.2023.124893
26. M. Sirajuddin, S. Ali, A. Badshah, Drug-DNA interactions and their study by UV-visible, fluorescence spectroscopies and cyclic voltametry. J. Photochem. Photobiol. B, Biol. **124**, 1–19 (2013). https://doi.org/10.1016/j.jphotobiol.2013.03.013
27. S.U. Rehman, T. Sarwar, M.A. Husain et al., Studying non-covalent drug-DNA interactions. Arch. Biochem. Biophys. **576**, 49–60 (2015). https://doi.org/10.1016/j.abb.2015.03.024
28. I. Kucuk, Ö.B. Küçükşahin, M. Yildirim et al., Investigation of the molecular interaction between apraclonidine, an α2-adrenergic receptor agonist, and bovine serum albumin using fluorescence and molecular docking techniques. Spectrochim. Acta A Mol. Biomol. Spectrosc. **326**, 125246 (2025). https://doi.org/10.1016/j.saa.2024.125246

29. M. Baginski, F. Fogolari, J.M. Briggs, Electrostatic and non-electrostatic contributions to the binding free energies of anthracycline antibiotics to DNA. J. Mol. Biol. **274**, 253–267 (1997). https://doi.org/10.1006/jmbi.1997.1399
30. Y. Gilad, H. Senderowitz, Docking studies on DNA intercalators. J. Chem. Inf. Model. **54**, 96–107 (2014). https://doi.org/10.1021/ci400352t
31. A. Khodadadi, E. Faghih-Mirzaei, H. Karimi-Maleh et al., A new epirubicin biosensor based on amplifying DNA interactions with polypyrrole and nitrogen-doped reduced graphene: experimental and docking theoretical investigations. Sens. Actuators, B Chem. **284**, 568–574 (2019). https://doi.org/10.1016/j.snb.2018.12.164
32. C. Erkmen, B. Bozal-Palabiyik, H. Tayyab et al., Exploring molecular interaction of cefpirome with human serum albumin: In vitro and in silico approaches. J. Mol. Struct. **1275**, 134723 (2023). https://doi.org/10.1016/j.molstruc.2022.134723
33. S. Rauf, J.J. Gooding, K. Akhtar et al., Electrochemical approach of anticancer drugs-DNA interaction. J. Pharm. Biomed. Anal. **37**, 205–217 (2005). https://doi.org/10.1016/j.jpba.2004.10.037
34. R. Nimal, D. Nur Unal, C. Erkmen et al., Development of the electrochemical, spectroscopic and molecular docking approaches toward the investigation of interaction between DNA and anti-leukemic drug azacytidine. Bioelectrochemistry **146**, 108135 (2022). https://doi.org/10.1016/j.bioelechem.2022.108135
35. X. Hai, Y. Li, C. Zhu et al., DNA-based label-free electrochemical biosensors: from principles to applications. TrAC Trends Anal. Chem. **133**, 116098 (2020). https://doi.org/10.1016/j.trac.2020.116098
36. M. Bilkay, C. Kanbes-Dindar, B. Bozal-Palabiyik et al., Spectroscopic, electrochemical, and molecular docking studies of the interaction between the antihistamine drug desloratadine and dsDNA. Anal. Biochem. **694**, 115622 (2024). https://doi.org/10.1016/j.ab.2024.115622
37. G.A. Evtugyn, A.V. Porfireva, S.V. Belyakova, Electrochemical DNA sensors for drug determination. J. Pharm. Biomed. Anal. **221**, 115058 (2022). https://doi.org/10.1016/j.jpba.2022.115058
38. B. Duman, C. Erkmen, M. Zahirul Kabir et al., In vitro interactions of two pesticides, propazine and quinoxyfen with bovine serum albumin: spectrofluorometric and molecular docking investigations. Spectrochim. Acta A Mol. Biomol. Spectrosc. **300**, 122907 (2023). https://doi.org/10.1016/j.saa.2023.122907
39. G. Rabbani, M.H. Baig, E.J. Lee et al., Biophysical study on the interaction between Eperisone hydrochloride and human serum albumin using spectroscopic, calorimetric, and molecular docking analyses. Mol. Pharm. **14**, 1656–1665 (2017). https://doi.org/10.1021/acs.molpharmaceut.6b01124
40. N. Shahabadi, N. Fatahi, M. Mahdavi et al., Multispectroscopic studies of the interaction of calf thymus DNA with the anti-viral drug, valacyclovir. Spectrochim. Acta A Mol. Biomol. Spectrosc. **83**, 420–424 (2011). https://doi.org/10.1016/j.saa.2011.08.056
41. L. Wang, Y. Wu, T. Chen, C. Wei, The interactions of phenanthroline compounds with DNAs: preferential binding to telomeric quadruplex over duplex. Int. J. Biol. Macromol. **52**, 1–8 (2013). https://doi.org/10.1016/j.ijbiomac.2012.08.015
42. W.M.F. Fabian, G. Kollenz, Y. Akcamur et al., Reaktionen cyclischer Oxalylverbindungen, 34. Mitt.: Synthese von Dibenzoylacet-N-carboxyalkylamiden und semiempirische Rechnungen zur Keto-Enol Tautomerie. Monatsh. Chem. **123**, 265–275 (1992). https://doi.org/10.1007/BF00810475
43. L.J. Farrugia, ORTEP -3 for Windows - a version of ORTEP -III with a graphical user interface (GUI). J. Appl. Crystallogr. **30**, 565–565 (1997). https://doi.org/10.1107/S0021889897003117
44. L.J. Farrugia, Wingx suite for small-molecule single-crystal crystallography. J. Appl. Crystallogr. **32**, 837–838 (1999). https://doi.org/10.1107/S0021889899006020
45. G.M. Sheldrick, A short history of SHELX. Acta Crystallogr. Sect. A Found. Crystallogr. **64**, 112–122 (2008). https://doi.org/10.1107/S0108767307043930
46. M. Gulcan, H. Zengin, M. Çelebi et al., 2, 6-Bis((E)-((5-benzoyl-2-thioxo-4-phenylpyrimidin-1(2H)-yl)imino)methyl)-4-(methyl)phenol and its metal(II) complexes: synthesis, spectroscopy, biological activity, and photoluminescence features. Z. Anorg. Allg. Chem. **639**, 2282–2289 (2013). https://doi.org/10.1002/zaac.201300224
47. M. Gulcan, U. Doğru, G. Öztürk et al., Fluorescence properties and electrochemical behavior of some Schiff bases derived from N-aminopyrimidine. J. Fluoresc. (2014). https://doi.org/10.1007/s10895-013-1303-x

48. M. Sönmez, M. Çelebi, İ Berber, Synthesis, spectroscopic and biological studies on the new symmetric Schiff base derived from 2,6-diformyl-4-methylphenol with N-aminopyrimidine. Eur. J. Med. Chem. **45**, 1935–1940 (2010). https://doi.org/10.1016/j.ejmech.2010.01.035
49. L. Álvarez, F. Brovelli, R. Baggio et al., Thione-thiol tautomeric equilibrium in a dihydropyrimidine-thione: X ray diffraction helped by NMR, FTIR and theoretical calculations. J. Chil. Chem. Soc. **67**, 5702–5707 (2022)
50. A.O. Sarıoğlu, Ü. Ceylan, ŞP. Yalçın et al., Synthesis of a new ONNO donor tetradentate schiff base ligand and binuclear Cu(II) complex: quantum chemical, spectroscopic and photoluminescence investigations. J. Lumin. **176**, 193–201 (2016). https://doi.org/10.1016/j.jlumin.2016.03.021
51. E. Paleček, M. Bartošík, Electrochemistry of nucleic acids. Chem. Rev. **112**, 3427–3481 (2012). https://doi.org/10.1021/cr200303p
52. M. Aslan, F. Aydın, F. Aslan, A. Levent, Application of disposable biosensor for Nivolumab–DNA interaction using pencil graphite electrode. Russ. J. Electrochem. **59**, 941–953 (2023). https://doi.org/10.1134/S1023193523110046
53. A. Erdem, Nanomaterial-based electrochemical DNA sensing strategies. Talanta **74**, 318–325 (2007). https://doi.org/10.1016/j.talanta.2007.10.012
54. D.E. Bayraktepe, A voltammetric study on drug-DNA interactions: kinetic and thermodynamic aspects of the relations between the anticancer agent dasatinib and ds-DNA using a pencil lead graphite electrode. Microchem. J. **157**, 104946 (2020). https://doi.org/10.1016/j.microc.2020.104946
55. Y. Song, D. Zhong, J. Luo et al., Binding characteristics and interactive region of 2-phenylpyrazolo[1,5- c]quinazoline with DNA. Luminescence **29**, 1141–1147 (2014). https://doi.org/10.1002/bio.2674
56. P. Singla, V. Luxami, R. Singh et al., Novel pyrazolo[3,4-d]pyrimidine with 4-(1H-benzimidazol-2-yl)-phenylamine as broad spectrum anticancer agents: synthesis, cell based assay, topoisomerase inhibition, DNA intercalation and bovine serum albumin studies. Eur. J. Med. Chem. **126**, 24–35 (2017). https://doi.org/10.1016/j.ejmech.2016.09.093
57. A. Wolfe, G.H. Shimer, T. Meehan, Polycyclic aromatic hydrocarbons physically intercalate into duplex regions of denatured DNA. Biochemistry **26**, 6392–6396 (1987). https://doi.org/10.1021/bi00394a013
58. A.R. Nekoei, M. Vatanparast, π-Hydrogen bonding and aromaticity: a systematic interplay study. Phys. Chem. Chem. Phys. **21**, 623–630 (2019). https://doi.org/10.1039/c8cp07003b

Authors and Affiliations

Nida Nur Adiyan[1] · Abdulkadir Levent[2] · Şerife Pınar Yalçın[3] · Mehmet Sönmez[4]

✉ Abdulkadir Levent
leventkadir@hotmail.com

Nida Nur Adiyan
nnursonmez@gmail.com

Şerife Pınar Yalçın
serifeyalcin@harran.edu.tr

Mehmet Sönmez
msonmez@gantep.edu.tr

[1] Department of Nutrition and Dietetics, Hasan Kalyoncu University, 27310 Gaziantep, Turkey

[2] Department of Analytical Chemistry, Faculty of Arts and Sciences, Batman University, 72100 Batman, Turkey

[3] Department of Physics, Faculty of Arts and Sciences, Harran University, 63000 Şanlıurfa, Turkey

[4] Department Chemistry, Faculty of Arts and Sciences, Gaziantep University, 27310 Gaziantep, Turkey